Acta Botanica Brasilica - 31(3): 344-357. July-September 2017.
doi: 10.1590/0102-33062016abb0279

A reduced, yet functional, nectary disk integrates a complex system of floral nectar secretion in the genus *Zeyheria* (Bignoniaceae)

Silvia Rodrigues Machado[1*], Camila Vaz de Souza[2] and Elza Guimarães[1]

Received: August 4, 2016
Accepted: October 21, 2016

ABSTRACT

The genus *Zeyheria* (Bignoniaceae) comprises only two species, both of which have been described as possessing a reduced and non-functional nectary disk. Despite the importance of this evolutionary change in the floral nectary, these functional assumptions have been based on disk size and on the distribution, abundance and histochemistry of corolla-borne trichomes. By combining methods on light and electron microscopy, here we investigated the functionality of the reduced nectary disk and describe all of the tissues and structures of the nectar chamber in order to determine the sites of floral nectar secretion in both *Zeyheria* species. . Our data find the floral nectary traits of both species to be very similar, although differing in their cellular contents. Subcellular evidence in both species indicated that disk, stipe and petal axils were, predominantly, involved in hydrophilic secretion, while capitate glandular trichomes produced lipophilic secretion and papillae produced mixed secretion. Our study shows that in spite of its reduced size, the reduced disk functions in nectar secretion in both species of *Zeyheria*. This kind of nectary system is a novelty for Bignoniaceae, since it comprises several tissues and structures functioning in an integrated fashion.

Keywords: Bignoniaceae, floral nectary, functional anatomy, histochemistry, ultrastructure

Introduction

Nectar is an aqueous solution produced by specialized structures (nectaries), largely distributed among angiosperms (Fahn 1979; Smets 1986; Nepi *et al*. 2009). The ontogenetic origin, size, shape or position of floral nectaries is variable among eudicotyledonous flowers (Pacini *et al*. 2003; Evert 2006; Bernardello 2007), and show no particular patterns associated with taxa, habitat or pollinator type (Herrera *et al*. 2006; Canto *et al*. 2007; Agostini *et al*. 2011; Wilmer 2011). Despite being referred to as a poorly elaborated carbohydrate-based solutions, nectar production requires extensive processing by the nectary cells, whose subcellular features reflect its final composition (Nepi 2007).

Nectar has been considered the most important resource available to anthophilous animals in angiosperms (Galetto & Bernardello 2005; Willmer 2011). Bignoniaceae species are predominantly zoophilous (Gentry 1974; Alcantara & Lohmann 2010) and the floral nectar production has been commonly attributed to a conspicuous nectary, characterized as a disk that surrounds the ovary base (Gentry 1992; Galetto 1995; 2009; Rivera 2000). This nectariferous disk is usually composed by a secretory

[1] Departamento de Botânica, Instituto de Biociências, Universidade Estadual Paulista, 18.618-970, Botucatu, SP, Brazil
[2] Programa de Pós-Graduação em Ciências Biológicas, Instituto de Biociências, Universidade Estadual Paulista, 18.618-970, Botucatu, SP, Brazil

* Corresponding author: smachado@ibb.unesp.br

epidermis and secretory parenchyma, predominantly supplied by phloem (Galetto 1995; Thomas & Dave 1992; Rivera 2000; Guimarães *et al*. 2016). However, in some genera as *Clytostoma*, *Cydista*, *Phryganocydia* (now treated as *Bignonia* according to Lohmann & Taylor 2014) and *Lundia* the nectariferous disk is absent, and these nectarless flowers are supposed to be pollinated by deceit (Gentry 1980). Remarkably, *Lundia cordata*, a Bignoniaceae species that possesses a vestigial and non-secretory disk, offers nectar as trophic resource, which production was assigned to the corolla-borne trichomes (Lopes *et al*. 2002). A similar pattern was described for *Zeyheria montana*, for which a functional disk is supposedly lacking (Gentry 1992) and floral nectar secretion was also attributed to the corolla-borne trichomes placed on the nectar chamber's inner corolla wall (Bittencourt & Semir 2004). So, for species in which the disk is absent or reduced, as *L. cordata* and *Z. montana,* the trichomes' carpet was considered as a substitute nectary (*sensu* Vogel 1997) considering that this type has evolved secondarily, after the disk lost its secretory function (Lopes *et al*. 2002; Bittencourt & Semir 2004). Despite the importance of this evolutionary change in the floral nectary in Bignoniaceae, these functional assumptions have been based only on disk size and on the distribution, abundance and histochemistry of corolla-borne trichomes in the nectar chamber. However, ultrastructural and chemical analyses are essential to investigate relationships between structure and cell functions (Fakan 2004).

Zeyheria genus is characterized as possessing a vestigial, non-functional nectary disk (Gentry 1992). This genus comprises only two species and both differ on their pollinators. *Zeyheria montana* is hummingbird-pollinated and produces copious diluted nectar (Bittencourt & Semir 2004), while *Z. tuberculosa* is bee-pollinated and produces a more concentrated nectar in smaller amounts (Souza 2015). Carrying-out a study on gynoecium secretory trichomes of *Zeyheria montana* (Machado *et al*. 1995; 2006) authors observed abundant starch grains in the reduced disk and presence of vascular tissues close to the disk. These observations led us to question the non-functionality of the reduced disk, since such attributes have been associated with nectar production (Fahn 1979; Nepi 2007). Additionally to the already described involvement of corolla-borne glandular trichomes in nectar secretion (Bittencourt & Semir 2004), we observed signs of secretory activity in other tissues and structures of the nectar chamber, which suggest that, in this species, floral nectary may comprise more than one site of secretion.

These observations motivated us to investigate, in a comparative way, the chemical and subcellular features of the reduced disk, aiming to determine its functionality, in both *Zeyheria* species since they differ in nectar volume and concentration. In addition, we investigated all the nectar chamber's tissues and structures in order to determine the functional role of each one and to characterize the floral nectary in both species.

Materials and methods

Plant species, sampling and study site

Zeyheria montana Mart. and *Z. tuberculosa* (Vell.) Bureau ex Verl. differ in relation to habit, type of vegetation, pollinators and nectar attributes (Gentry 1992; Rizzini 1997). *Zeyheria montana* is a typical shrubby species, hummingbird-pollinated with diluted and copious nectar, that occurs in the Brazilian savanna (Bittencourt & Semir 2004). *Zeyheria tuberculosa* is a tree species, bee-pollinated with little and more concentrated nectar that occurs in seasonal semi deciduous forests in Brazil (Souza 2015).

This study was conducted from 2008 to 2015 on five adult specimens of *Z. montana* and five of *Z. tuberculosa* growing in savanna and forest areas, respectively, at Botucatu municipality, São Paulo State, Brazil (22°55'S 48°30'W). Anthesis in *Z. montana* lasted about six days and around four days in *Z. tuberculosa* and in both species nectar production started in pre-anthesis buds. From each individual four pre-anthesis buds and four first-day functional flowers (n = 20 samples per species), both stages showing nectar production, were collected. The flowers were observed and dissected under a stereomicroscope. Then, 20 samples of each stage were fixed for anatomical (five samples) and histochemical (five samples) studies on light microscopy (LM) and for ultrastructural studies on scanning (SEM) (five samples) and transmission (TEM) (five samples) electron microscopy.

Voucher of *Z. montana* (number 28469-28470) and of *Z. tuberculosa* (number 30818-30819) are deposited on BOTU Herbarium.

Scanning electron microscopy (SEM)

For SEM, the samples (n = 10 plants) were fixed in 2.5% glutaraldehyde (GA) in 0.1 M phosphate buffer (pH 7.2), dehydrated in an ethanol series, dried by the critical point method using liquid CO_2, and sputter-coated with approximately 10 nm of gold (Robards 1978). The materials were observed in a FEI Quanta 200 SEM (FEI, Hillsboro, OR, USA) at 20 kV.

Light microscopy (LM)

For LM, the samples were fixed in FAA 50 (formaldehyde, acetic acid, and 50% ethanol 1:1:18 v/v) (Johansen 1940), dehydrated in an ethanol series, and embedded in methylmethacrylate-based resin. Semi-thin sections (5-6 µm) were cut with disposable steel razors on a RM2255 (Leica) rotary microtome, mounted on glass slides and stained with 0.05% Toluidine Blue O (pH 4.3) (O'Brien *et al*. 1964). Fresh hand-cut sections and semi-thin sections were treated with Sudan III (Johansen 1940) for total lipids;

Lugol's reagent for starch grains (Johansen 1940); NADI reagent for terpenes (David & Carde 1964); Dragendorff reagent for alkaloids (Svendsen & Verpoorte 1983); mercuric bromophenol blue to detect total proteins (Mazia *et al*. 1953); Fehling's solution to detect reducing sugars (Purvis *et al*. 1964). Samples treated with aluminium trichloride and lead neutral acetate (Charrière-Ladreix 1976) were analysed under fluorescence microscope for flavonoids. Standard control procedures were carried out simultaneously. Starch grains and calcium oxalate crystals were detected using polarized light. The preparations were examined and photographed using an Olympus BX-51 microscope (Olympus, Tokyo, Japan) with Image-ProExpress software (Media Cybernetics Inc., Silver Spring, Maryland, USA).

Transmission electron microscopy (TEM)

For conventional ultrastructural analysis, samples of pre-anthesis buds and first-day functional flowers were fixed in glutaraldehyde (2.5% with 0.1 M phosphate buffer, pH 7.3, for 6–8 h at 4 °C), post-fixed with 1% osmium tetroxide (O_sO_4) aqueous solution in the same buffer, for 2h at room temperature. Samples were then dehydrated using a graded acetone series and embedded in Araldite resin at room temperature. Polymerization was performed at 60 °C for 48 h. Ultra-thin sections were stained with uranyl acetate and lead citrate (Reynolds 1963), and examined with a TEM Tecnai Spirit (FEI) at 60 kv. In addition, samples were treated with ZIO method (zinc iodide–osmium tetroxide) to improve the visualization of endomembranes (Reinecke & Walther 1978).

Results

The micromorphology, histochemistry, anatomy and ultrastructure of the reduced disk and of all the other tissues and structures that comprise the nectar chamber were characterized in this study. The similar results are presented for the two studied *Zeyheria* species and the differences between them were highlighted in the text. Additionally, due to anatomical, histochemical and ultrastructural similarities, the data from disk and stipe were grouped and presented together. As no differences were found in any of the secretory tissues and structures between pre-anthesis and first-day functional flowers, the results were presented only for functional flowers.

Nectar chamber micromorphology

Both *Zeyheria* species had similar nectar chamber morphology (Fig. 1), showing four regions with secretory features: the reduced disk (Fig. 2), the stipe (Fig. 3), the petals' axils (Fig. 4) and the floral tube internal wall (Figs. 5, 6).

The tubular flowers of both Zeyheria species accumulated nectar, since pre-anthesis stage, in a chamber located at the base of the floral tube, which was delimited by an upper constriction formed by the thickened bases of epipetalous filets disposed around the ovary (Fig. 1A).

The reduced nectary disk, in both species of *Zeyheria*, was flattened, protuberant, and occurred at the base of the stipe (Fig. 1A-C), but in *Z. montana* it was more conspicuous (Fig. 1B). The disk's surface was sparsely covered with trichomes in both species (Fig. 1B-C), while the stipe was densely covered by glandular and non-glandular trichomes (Fig. 1A-C). In both species, prominent modified stomata were distributed throughout the disk's surface and remnants of the flocculent secretion could be observed especially around the stomata (Fig. 1D). The inner surface of the nectar chamber was lined with glandular capitate-type trichomes (Fig. 1A, E-H) distributed among papillae (Fig. 1F-G), except on the corolla tube's base, which was glabrous (Fig. 1E). The papillae exhibited variable sizes and verrucose cuticle (Fig. 1F-G). Cuticle blisters resulting from subcuticular secretion accumulation in the distal region of the capitate trichomes' head cells (Fig. 1H) were registered since the pre-anthesis stage.

Histochemistry

The histochemical tests revealed the presence of flavonoids, starch grains, reduced sugars, terpenes/ resin and total lipids in both species (Tab. 1). Disk-stipe and petal's axil reacted positively for starch grains, reduced sugars, and total lipids. Only capitate trichomes' head cells reacted positively to terpenes/ resin and total lipids tests. Papillae reacted positively to total flavonoids and lipids. Proteins were detected only in *Z. montana*, which occurred in the disk-stipe and papillae.

Nectar chamber histology and ultrastructure

The reduced disk (Fig. 2) and the stipe (Fig. 3) were composed by a uniseriate epidermis and covered by a thin cuticle, a nectary parenchyma formed by isodiametric and compactly arranged voluminous cells, and a subnectary parenchyma constituted by larger loosely arranged cells and vascularized mainly by phloem, showing well-developed intercellular spaces (Fig. 2A). Xylem was abundant in the junction of the disk's base to the petals' axils (Fig. 2A).

By TEM, both epidermal and parenchyma cells of the disk (Fig. 2B) and stipe (Fig. 3A) presented similar features. In both *Zeyheria* species these cells had conspicuous nuclei with evident nucleolus, abundant cytoplasm and vacuoles of variable sizes (Figs. 2B, 3A). Big starch grains occurred in all the disk and stipe cells showing a clear decrease in abundance and size from the parenchyma towards the epidermis (Figs. 2B, 3A-C). Epidermal and parenchyma cells exhibited dense cytoplasm with abundant ribosomes (Figs.

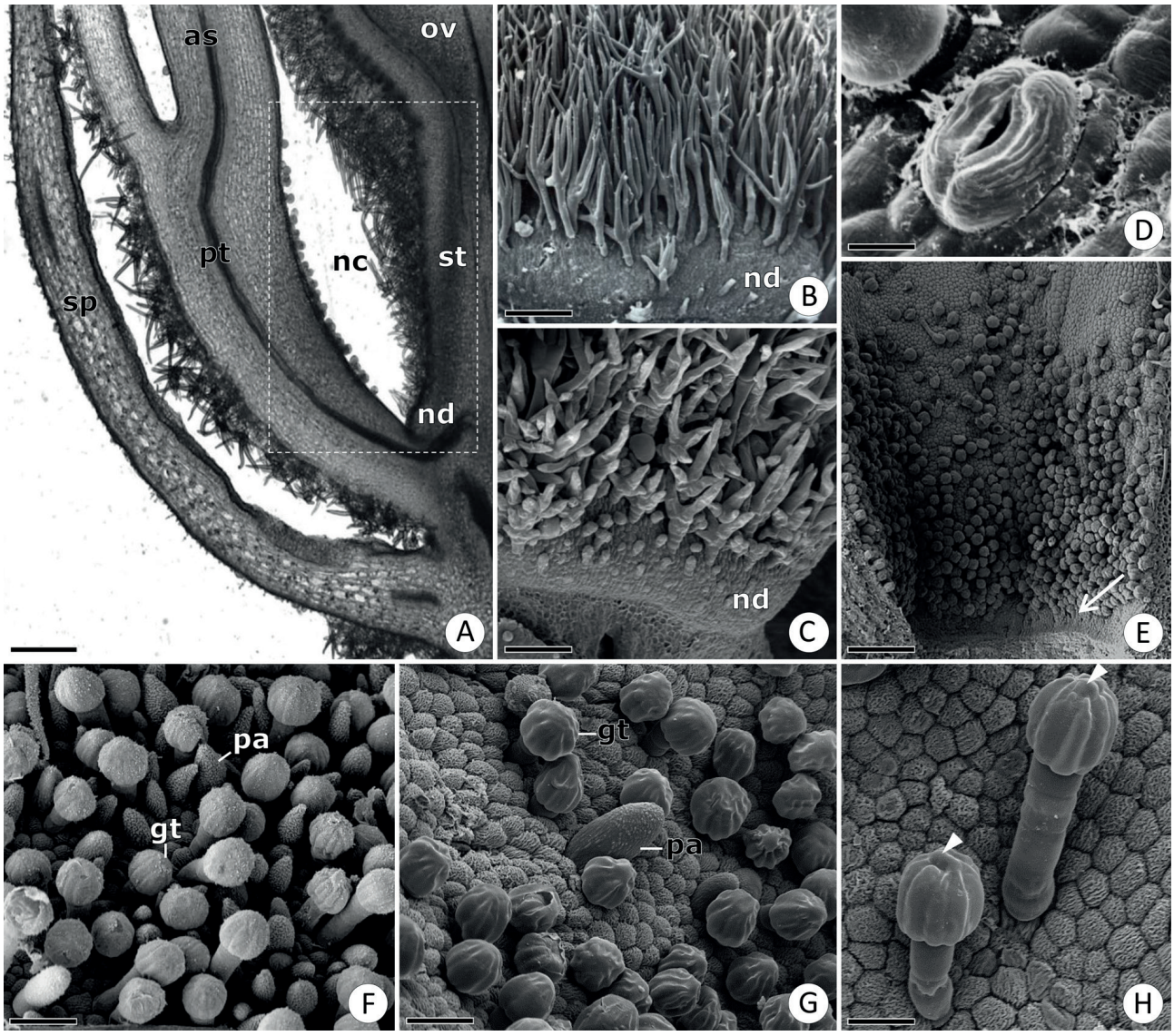

Figure 1. Characterization of *Zeyheria montana* and *Z. tuberculosa* nectar chamber. (A = Light microscopy, B-H = SEM). (A) Longitudinal section through basal portion of the flower tube of *Z. tuberculosa* showing the nectar chamber (hatched area) that comprises the reduced nectary disk, the stipe covered with abundant ramified non-glandular trichomes, the petals axil and the base of corolla covered with abundant glandular trichomes. (B) Glabrous nectary disk in *Z. montana*. (C) Glabrous nectary disk in *Z. tuberculosa*. (D) Stomata on the nectary disk in *Z. montana*, note the flocculent material around the stomata. (E) Corolla base of *Z. tuberculosa* showing the glabrous petal's axils (arrow) and the upper region lined with glandular trichomes. (F) Detail of the nectar chamber showing the capitate glandular trichomes and papillae in *Z. montana*. (G) Detail of the nectar chamber showing the capitate glandular trichomes and papillae in *Z. tuberculosa*. (H) Detail of the capitate glandular trichomes of variable sizes showing the cuticle blisters (arrow head) in the apical region of secretory head in *Z. tuberculosa*. Scale bars = 200 μm (A), 100 μm (B, C), 20 μm (D), 150 μm (E), 50 μm (F, G), 25 μm (H). **Abbreviations**: as, adnate stamen; gt, glandular trichome; nc, nectar chamber; nd, nectary disk; ov, ovary; pa, papilla; pt, petal; sp, sepal; st, stipe.

2C, 3B), mitochondria (Figs. 2D, 3B), endoplasmic reticulum (Figs. 2F-H, 3B, G), Golgi bodies (Figs. 2D, G, I, 3B-D) and round plastids (Figs. 2B-C, 3A-C), which contained big starch grains and lipid droplets in both species, and protein bodies in *Z. montana* (Fig. 2C). Plastids with residual starch grains occurred in subepidermal parenchyma cells (Fig. 3E). Endoplasmic reticulum (Fig. 2G-H) and Golgi bodies and associated vesicles (Figs. 2G, I, 3C-D) were better viewed with the use of the ZIO method. In addition, parenchyma and epidermal cells showed juxtaposed vesicles with plasma membrane (Figs. 2F, 3G), cytoplasmic oil bodies (Figs. 2E, H, K, 3C, E, G), and multivesicular bodies (Fig. 2F, J). Protein bodies were abundant in *Z. montana* disk and stipe cells, occurring inside plastids (Fig. 2C) and scattered in the cytoplasm (Fig. 2C, J), while these inclusions were absent in *Z. tuberculosa*. The vacuoles contain finely flocculent

Table 1. Histochemistry of nectar chamber tissues and structures from first day flowers of *Zeyheria montana* (*Z. m.*) and *Z. tuberculosa* (*Z. t.*) (Bignoniaceae).

Reagents	Target compounds	Colour	Disk and stipe		Petals' axil		Capitate trichomes		Papillae	
			Z. m.	*Z. t.*	*Z. m.*	*Z. t.*	*Z. m.*	*Z. t.*	*Z. m.*	*Z. t.*
Dragendorff	Alkaloids	Brownish	-	-	-	-	-	-	-	-
Lead neutral acetate	Flavonoids	Yellowish	-	-	-	-	-	-	+	+
Mercuric bromophenol blue	Proteins	Blue	+	-	-	-	-	-	+	-
Lugol	Starch grains	Black	+	+	+	+	-	-	-	-
Fehling	Sugars	Reddish	+	+	+	+	-	-	-	-
NADI	Terpenes/ resins	Violet-blue	-	-	-	-	+	+	-	-
Sudan III	Total lipids	Orange-red	+	+	+	+	+	+	+	+

- negative, + positive

material (probably the polysaccharides previously detected with histochemical tests) and electron-lucent material (oils), besides membranous material (Figs. 2E, J, K, 3E, G). Sieve tube elements of large calibre with companion and parenchyma cells were registered in the parenchyma of the disk and stipe (Fig. 2L; 3F). Wall protuberances coated with the plasma membrane were observed on the entire inner wall surface of the stipe parenchyma cells (Fig. 3B). The anticlinal walls of epidermal cells showed primary pit fields with abundant plasmodesmata (Fig. 2E, M). Accumulations of dense material traversing the inner and outer periclinal walls, in the cytoplasm and vacuoles besides lipid drops on the cuticle surface were commonly observed in epidermal cells (Fig. 2M). Developed periplasmic space containing dense or flocculent material was observed in the epidermal (Fig. 2F, M) and parenchyma cells (Figs. 2G, 3E, G). Intercellular spaces, variable in extension and width, filled with finely flocculated material (polysaccharides), were observed in the parenchyma tissue (Figs. 2N, 3G).

The petals' axils (Fig. 4) exhibited uniseriate epidermis composed by small cells irregular in shape, covered by a smooth and thin cuticle, and subepidermal parenchyma composed by compactly arranged small cells of various shapes (Fig. 4A). Ultrastructurally, epidermis and parenchyma cells were characterized by presenting thickened walls, conspicuous nuclei, dense cytoplasm and vacuoles of different sizes (Fig. 4B). Amyloplasts filled with conspicuous starch grains (Fig. 4B-C), endoplasmic reticulum (Fig. 4D-F), hyperactive well-developed Golgi bodies (Fig. 4C-D) and mitochondria (Fig. 4C) were the most evident organelles in these cells. Conspicuous oil bodies occurred scattered in the cytoplasm (Fig. 4D, F). The vacuoles presented flocculent material and membrane debris (Fig. 4C). Images of vesicle juxtaposed to the plasma membrane (Fig. 4D), which was sinuous in outline (Fig. 4D-F), were frequently observed in these cells. Flocculent material occurred in the periplasmic space of those cells (Fig. 4D-F). Just in the petal junction to the disk, the thickness of epidermal cells' walls was remarkable (Fig. 4E). The swelling of the middle lamellae and its posterior dissolution along the anticlinal walls of the epidermal cells originated channels that exhibited accumulated secretion (Fig. 4E).

The glandular capitate trichomes (Fig. 5) were composed by an epidermal basal cell, a uniseriate stalk formed by 1-5 cells, and a secretory head with 12-24 cells concentrically disposed in one or two layers. Trichomes, with a variable number of cells in the stalk and secretory head, occurred side-by-side (Fig. 1F-H). The glandular trichomes were covered with a thick cuticle that was thicker on the lateral walls of the stalk cells (Fig. 5A-B). Cuticle blisters, originated by the secretion accumulation between the cell walls and cuticle, were more evident in the distal pole of the secretory head (Figs. 1H, 5B, G). Prior to the accumulation of secretion in the subcuticular space, the outer periclinal walls of the head cells showed a homogenous polysaccharide inner stratum that was followed by a dense intermediate fibrous layer, which protruded towards the cuticle layer forming a network of electron-dense ramifications in this cuticle region (Fig. 5C). The dissolution of the intermediate polysaccharide layer preceded the cuticle detachment from the outer cell wall (Fig. 5F). The cells from the secretory head showed a central and spherical nucleus, vacuoles of variable sizes and shapes, and dense, abundant cytoplasm (Fig. 5A-B). Polyribosome (Fig. 5C, E-F), globular mitochondria with a well-developed cristae (Fig. 5F, G), scarce Golgi bodies (Fig. 5E), extensive profiles of rough endoplasmic reticulum (Fig. 5F) and dilated smooth endoplasmic reticulum (Fig. 5C, G), and modified plastids (Fig. 5G-I) characterized the cytoplasm of the head cells. The plastids were large, round (Fig. 5H) or oval (Fig. 5I) and filled with tubular electron-dense structures and osmiophilic inclusions of different sizes. In the head cells, it was remarkable the abundance of scattered electron-lucent droplets (Fig. 5D) and electron-dense inclusions (Fig. 5D-H), previously identified as lipids. Some head cells exhibited a developed periplasmic space with irregular contour and accumulations of heterogeneous materials (Fig. 5F-G, I). These cells had sinuous walls with a loose aspect (Fig. 5F). Subcuticular space occurred through all the extension of the head cells (Fig. 5B, F), although it was more developed in the apical pole of the secretory head (Fig. 5B, G). The subcuticular space contained abundant lipid accumulations and some flocculated material (Fig. 5G).

Papillae (Fig. 6) were covered with a thick and folding cuticle forming tall, deep sulci at the cell surface (Fig. 6A).

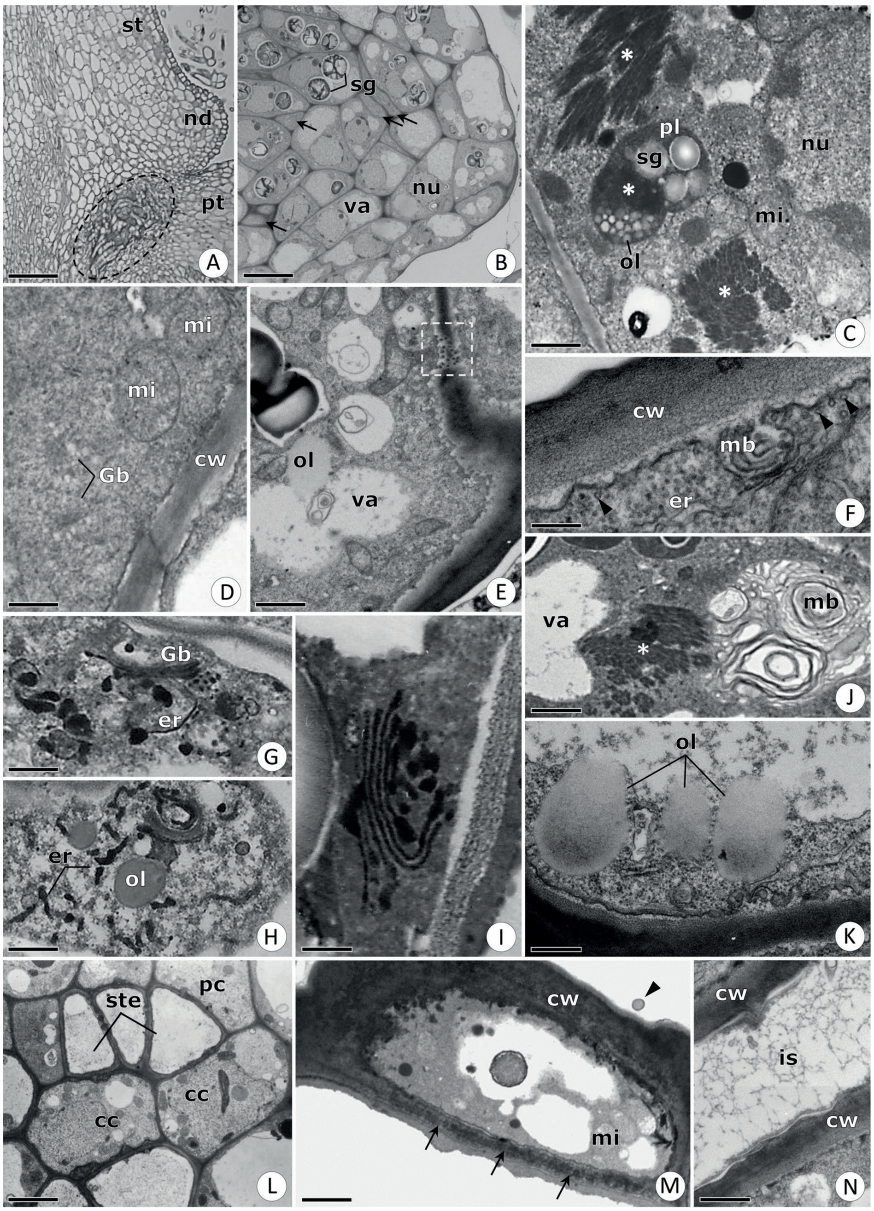

Figure 2. Nectary disk of *Zeyheria montana* and *Z. tuberculosa* flowers in the first day of anthesis. (A = Light microscopy, B-N = TEM). (A) Longitudinal section through the *Z. tuberculosa* corolla tube base showing the nectary disk composed by uniseriate epidermis and nectary parenchyma. The hatched area shows abundant xylem in the junction region of corolla base and nectary disk. (B) A general view of *Z. tuberculosa* disk showing the uniseriate epidermis and nectary parenchyma cells with conspicuous nuclei, vacuoles of variable sizes, starch grains and phloem elements. Note that starch grains decreased in size and abundance from nectary parenchyma toward epidermis. (C) Nectary parenchyma cell of *Z. montana* showing plastids containing starch grains, protein inclusions an oil drops and protein bodies scattered in the cytoplasm (*). (D) Nectary parenchyma cell of *Z. montana* showing hyperactive Golgi bodies and mitochondria. (E) Epidermal cells of *Z. tuberculosa* disk showing vacuoles filled with finely flocculent material, oil bodies and membrane debris. Note abundant plasmodemata in the hatched area. (F) Epidermal cells of *Z. tuberculosa* disk showing sinuous plasma membrane, abundant ribosomes, and endoplasmic reticulum and mutivesicular bodies. Note vesicles (head arrows) close to the plasma membrane. (G, I) Golgi bodies and vesicles and (G, H) tubules of endoplasmic reticulum marked with ZIO methods in the nectary parenchyma cells of *Z. montana*. (J) Nectary parenchyma cell of *Z. montana* exhibiting vacuole with multivesicular bodies and protein inclusions in the cytoplasm. (K) Oil bodies in the epidermal cells of *Z. tuberculosa*. (L) Phloem cells in the nectary parenchyma of *Z. montana*. (M) Epidermal cell of *Z. tuberculosa* with dense accumulations in the walls and periplasmic space, oil drops scattered in the cytoplasm and on the cuticle (arrow head). Arrows indicate plasmodesmata in the inner periclinal cell wall. (N) Intercellular space with accumulations of flocculent material in the nectary parenchyma of *Z. tuberculosa*. Scale bars = 150 µm (A), 5 µm (B), 0,5 µm (C, G, H, J, N), 0,4 µm (D, I), 0,7 µm (E), 0,2 µm (F, K), 2 µm (L), 1,5 µm (M). **Abbreviations:** cc, companion cells; cw, cell wall; er, endoplasmic reticulum; Gb, Golgi body; is, intercellular space; mb, multivesicular body; mi, mitochondria; nd, nectary disk; nu, nuclei; ol, oil body; pc, parenchyma cells; pl, plastid; pt, petal; sg, starch grains; st, stipe; ste, sieve tube elements; va, vacuole.

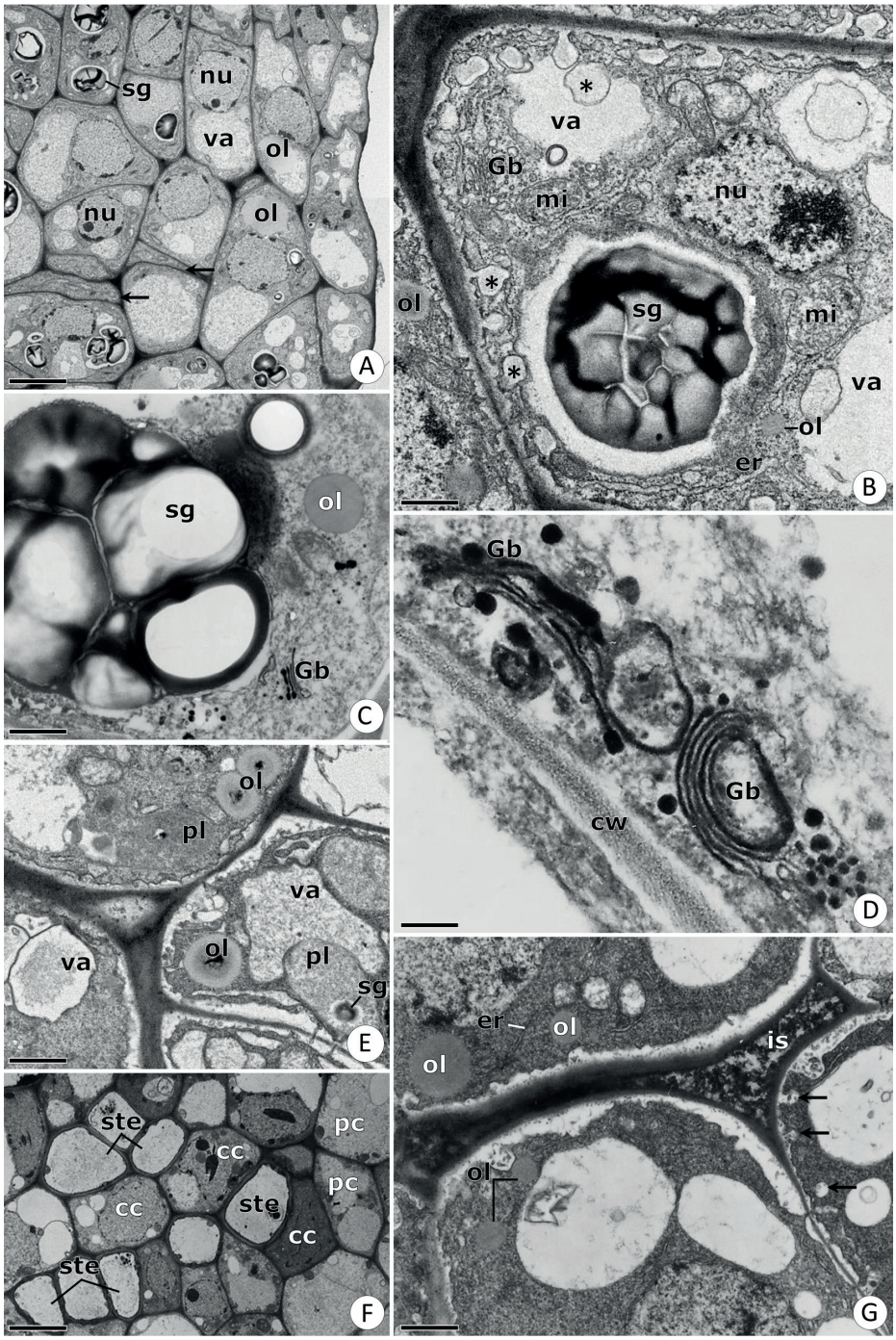

Figure 3. Stipe of *Zeyheria montana* and *Z. tuberculosa* flowers in the first day of anthesis (TEM). *Z. tuberculosa* (A-B, E-G) and *Z. montana* (C-D). (A) A general view of the epidermis and parenchyma cells with conspicuous nuclei (nu), vacuoles of variable sizes, oil bodies, and amyloplasts with starch grains. Arrows indicate phloem elements. Note that the starch grains decreased in size and abundance from nectary parenchyma toward epidermis. (B) Detail of parenchyma cells showing nuclei, Golgi bodies, mitochondria, endoplasmic reticulum, plastid with large starch grains and vacuoles containing finely flocculent material and membrane debris. Note the wall protuberances (*). (C) Detail of cytoplasm from the parenchyma cell showing Golgi body, amyloplasts and oil drop. (D) Golgi bodies cisterns and vesicles marked with ZIO method. (E) Subepidermal parenchyma cells showing cytoplasmic oil bodies, plastids with residual starch grains and vacuoles filled with flocculent material. (F) Phloem comprised by sieve tube elements with large caliber, companion cells and parenchyma cells. (G) Parenchyma cells with abundant ribosomes, extensive endoplasmic reticulum, cytoplasmic oil bodies, and developed periplasmic space. Observe vesicles merged with plasma membrane (arrows) and intercellular space filled with flocculent content. Scale bars = 4 μm (A, F), 0,5 μm (B, C), 0,4 μm (D), 1 μm (E), 0,8 μm (F). **Abbreviations**: cc, companion cells; cw, cell wall; er, endoplasmic reticulum; Gb, Golgi body; is, intercellular space; mi, mitochondria; nu, nuclei; ol, oil body; pc, parenchyma cells; pl, plastid; sg, starch grains; ste, sieve tube elements; va, vacuole.

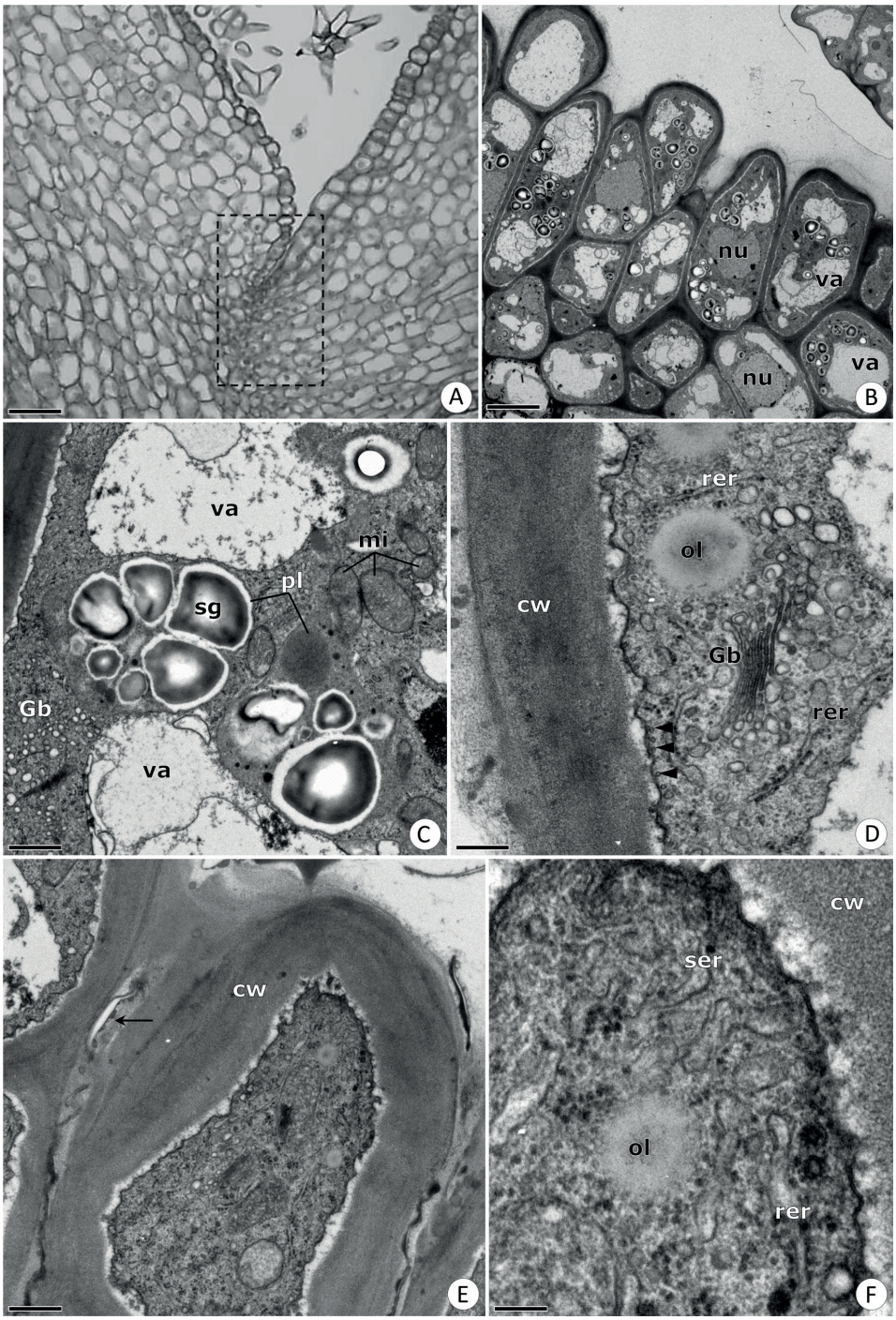

Figure 4. Petals' axils of *Zeyheria tuberculosa* flowers in the first day of anthesis. (A = Light microscopy, B-F = TEM). (A) Longitudinal section trough the corolla tube base showing the petal's axils (hatched area) comprised by smaller epidermal and parenchyma cells, compactly arranged. (B) A general view showing epidermis and parenchyma cells of variable size and shape with conspicuous nuclei, dense cytoplasm with amyloplasts, and vacuoles of variable sizes. (C) Detail of epidermal cell showing plastids containing starch grains of variable sizes, mitochondria and Golgi body. Note the vacuoles presenting flocculent materials and membrane debris. (D) Detail of cytoplasm of epidermal cell showing RER profiles, hyperactive Gogi bodies with numerous adjacent vesicles and conspicuous oil bodies. Note the vesicles close to the plasma membrane (arrowhead). (E) Epidermal cell in the junction of the petal and the disk presenting a very thick cell wall, dense and abundant cytoplasm rich in membranous organelles. Note the formation of channels in the thickened middle lamellae along the anticlinal cell walls (arrows). (F) Detail of the previous figure showing cytoplasmic oil body, polyribosomes, proliferate RER and SER, vesicles close to the plasma membrane and flocculent material in the periplasmic space. Scale bars: 80 µm (A), 5 µm (B), 2 µm (C) 1 µm (D), 2,5 µm (E), 0,5 µm (F). Abbreviations: cw, cell wall; Gb, Golgi body; mi, mitochondria; nu, nuclei; ol, oil body; pl, plastid; rer, rough endoplasmic reticulum; ser, smooth endoplasmic reticulum; sg, starch grains; va, vacuole.

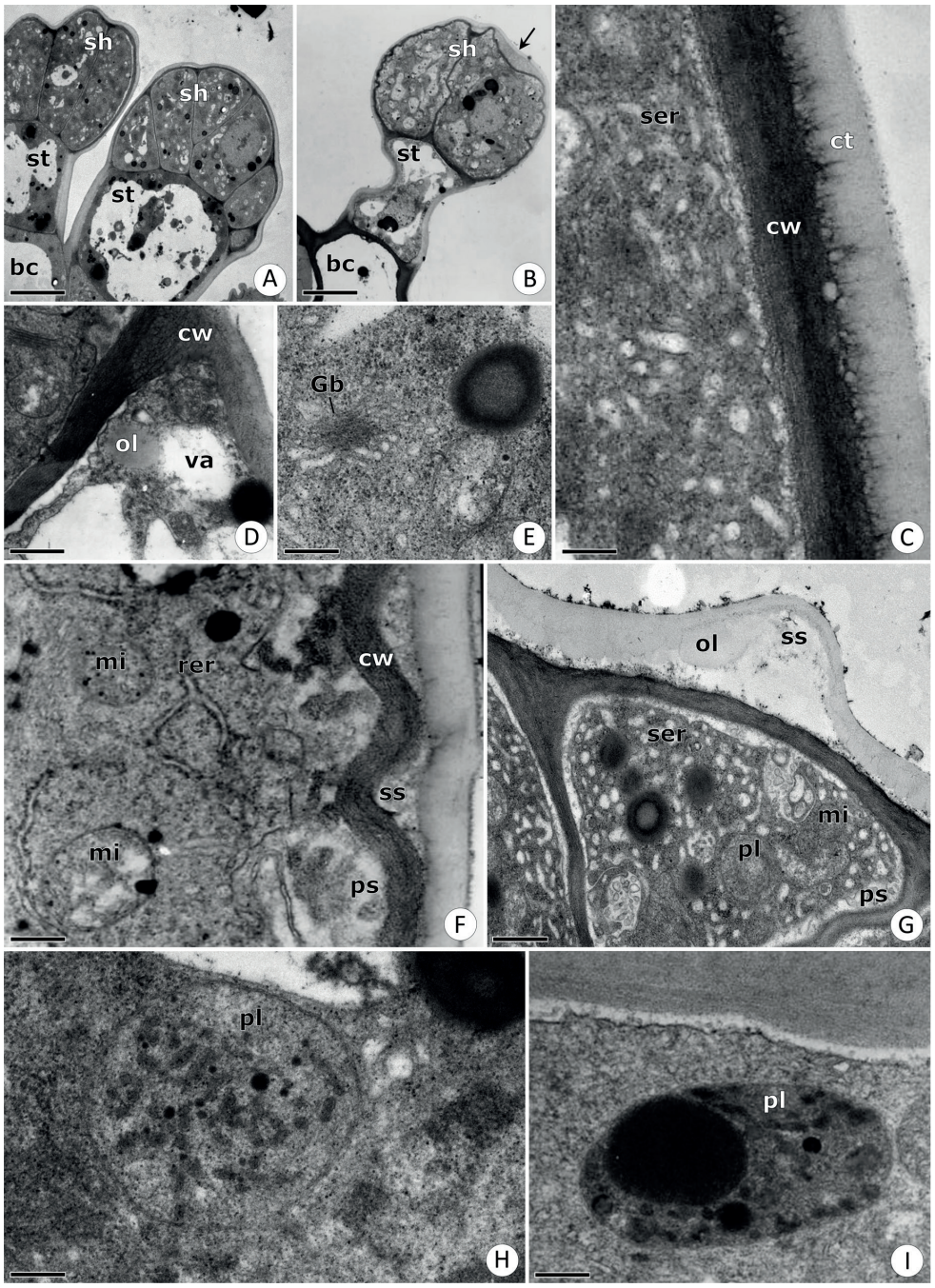

Figure 5. Capitate trichomes of *Zeyheria montana* and *Z. tuberculosa* flowers in the first day of anthesis (TEM). (A-B) A general view of the capitate trichomes showing the basal cell, wide stalk cell and secretory head covered with a thick cuticle of *Z. tuberculosa* and *Z. montana*, respectively. Note the subcuticular space (arrow) in the apical region of the secretory head in (B). (C) Detail of *Z. tuberculosa* head cell showing the thick cuticle presenting a cuticle layer containing a dense fibrillar network. Note abundant and dilated smooth endoplasmic reticulum in the cytoplasm. (D) Detail of *Z. montana* head cell showing electron-lucent and electron-dense bodies in the cytoplasm. (E) Part of cytoplasm of *Z. tuberculosa* head cell showing abundant polyribosomes, Golgi body and electron-dense inclusion. (F) Detail of head cell of *Z. montana* showing sinuous loose cell wall and secretion accumulated in the subcuticular and periplasmic space. Note extensive RER and globular mitochondria in the cytoplasm. (G) Apical region of secretory head of *Z. tuberculosa* showing the proliferated SER with dilated cisterns. Note the presence of globular plastids, cytoplasmic dense bodies and mitochondria. Observe the large periplasmic space and subcuticular space with oil accumulation. (H-I) Globular plastid with electron-dense tubules and dark granules in the stroma in *Z. tuberculosa* and Z. montana, respectively. Scale bars = 5 μm (A, B), 0,5 μm (C, H-I), 1 μm (D), 0,7 μm (E, F), 2 μm (G). **Abbreviations**: bc, basal cell; ct, cuticle; cw, cell wall; Gb, Golgi body; mi, mitochondria; ol, oil body; pl, plastid; ps, periplasmic space; rer, rough endoplasmic reticulum; st, stalk cell; sh, secretory head; ser, smooth endoplasmic reticulum; ss, subcuticular space; va, vacuole.

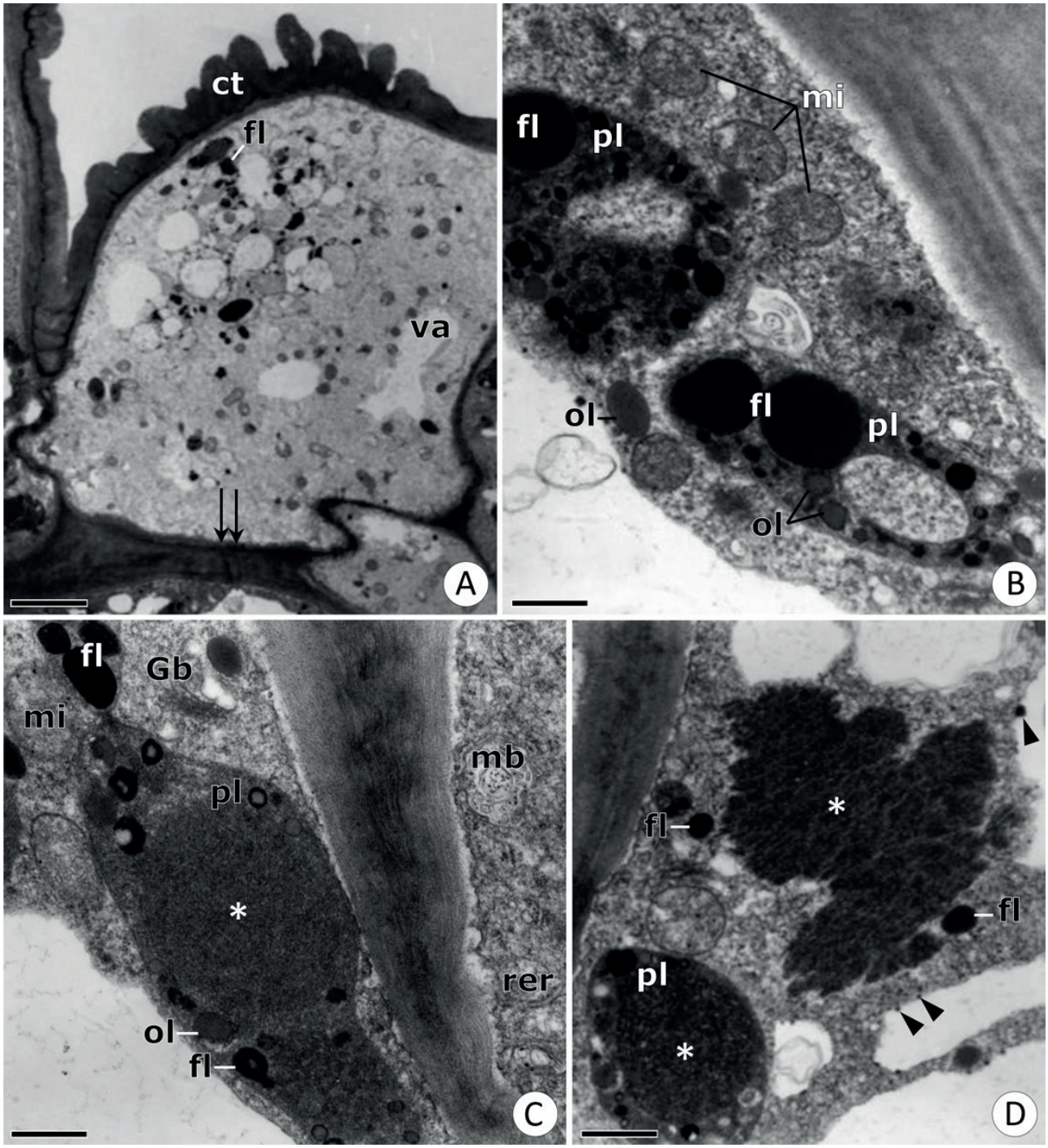

Figure 6. Papilla of *Zeyheria montana* flowers in the first day of anthesis (TEM). (A) A general view of the papilla showing thick folding cuticle, abundant cytoplasm, small vacuoles and cytoplasmic dense inclusions, previously identified as flavonoids. Arrows indicate Plasmodesmata in the inner periclinal cell wall. (B) Detail of cytoplasm exhibiting polyribosomes, globular mitochondria containing black granulations, plastids with electron-dense inclusions, and scattered oil drops. (C) Part of two cells showing dense cytoplasm with Golgi body, mitochondria, rough endoplasmic reticulum, multivesicular bodies and plastid containing protein inclusion (*), osmiophilic granulations and oil inclusion. Note rough endoplasmic reticulum profiles juxtaposed to the plasma membrane. (D) Conspicuous protein bodies in the cytoplasm and inside plastid (*). Note flavonoids scattered in the cytoplasm and attached to the inner surface of the tonoplast. Scale bars = 3 µm (A), 0,7 µm (B, D), 0,5 µm (C). Abbreviations: ct, cuticle; fl, flavonoid; Gb, Golgi body; mb, multivesicular body; mi, mitochondria; ol, oil bodies; pl, plastid; rer, rough endoplasmic reticulum; va, vacuole.

These cells exhibited sinuous thin walls interconnected by abundant plasmodesmata (Fig. 6A). Cytoplasm was abundant (Fig. 6A) and rich in polyribosomes, globular mitochondria, plastids (Fig. 6B-D), Golgi bodies, rough endoplasmic reticulum and multivesicular bodies (Fig. 6C). Mitochondria showed well-developed cristae and black granulations (Fig. 6C). Plastids lacking inner membrane and exhibiting inclusions of different aspects, including deeply electron-dense bodies (flavonoids), electron-lucent drops (oils) and granular material (proteins) were registered (Fig. 6B-D). Figures suggesting the fusion of rough endoplasmic reticulum profiles with the plasma membrane were commonly registered (Fig. 6C). Osmiophilic bodies, previously identified as flavonoids, occurred inside plastids (Fig. 6B-D), attached to the inner tonoplast surface (Fig. 6D) and scattered through the cytoplasm (Fig. 6A, D). Conspicuous protein bodies occurred inside plastids (Fig. 6C-D) and scattered through the cytoplasm (Fig. 6D).

Discussion

Our data support that the reduced disk, stipe, petals' axils, glandular trichomes and papillae have subcellular evidences of secretory activity. In both species, disk, stipe and petals' axils are involved in hydrophilic secretion, while capitate glandular trichomes in lipophilic secretion and papillae in mixed secretion. We present strong evidence that although reduced in size, the nectary disk is functional in nectar secretion in both *Zeyheria* species. It is important to emphasize that the disk-stipe differ in the cellular contents. In *Z. montana* proteins are predominant, while in *Z. tuberculosa* lipids droplets are more abundant. Lipids and proteins, or their derivatives, as amino acids, have been described as nutritionally valuable nectar componentes that contribute to its attractiveness for various mutualistic animals (Baker & Baker 1983; González-Teuber & Heil 2009).

Our study clearly showed that the disk, in spite of the reduced dimensions, has a functional vascularized parenchyma that storages and hydrolyses starch, besides presenting typical cellular features associated to nectar-producing tissues, including large mitochondria, rough endoplasmic reticulum (RER), well-developed Golgi bodies and abundant vesicles (Fahn 1979; 1988; Roshchina & Roshchina 1993; Nepi 2007). These evidences show that the disk in the *Zeyheria* genus is functional in nectar secretion. This finding differ from Bittencourt & Semir (2004) that referred the disk in flowers of *Z. montana* as vestigial, non-functional and ascribing nectar secretion to the corolla-borne glandular trichomes.

As both, disk and stipe, were similar in ultrastructure and histochemistry we considered them as a functional unity involved in nectar secretion, herein called 'disk-stipe'. We hypothesized that nectar production in the stipe may compensate for the disk's reduced size, since there is a considerable increase in area of tissues with secretory activity. In fact, a considerable amount of nectar is produced from the pre-anthesis buds, mainly in *Z. montana* (Machado *et al*. 2006). Nectar release may occur through modified stomata placed only at the disk, similar to what is reported for other Bignoniaceae species (Guimarães *et al*. 2016) and through the intact cuticle, as reported by Nepi (2007) for several other plant species, since we didn't find cuticle pores. The dense trichomes coverage in the stipe did not allow us to verify the occurrence of modified stomata in this region. The presence of amyloplasts with voluminous starch grains was remarkable in the disk-stipe parenchyma cells of both *Zeyheria* species. These starch grains showed a gradual reduction in size and in abundance from the parenchyma cells toward the epidermis. Other authors, like Nepi (2007 and references therein) have described a similar pattern in different species and believe that starch grains' hydrolysis in the nectary parenchyma contributes directly to nectar carbohydrate's supply, which reinforces our findings about the disk-stipe functionality. We detected an abundance of proteins in the cellular contents of *Z. montana*. In fact, proteins and amino acids were detected in the floral nectar of this plant species (E. Guimarães unpubl. res.). The presence of proteins in nectar has been registered since the 1930's and several functions have been ascribed to them (Beutler 1935; Pryce-Jones 1944; Baker & Baker 1975). The proteins and amino acids registered in the floral nectar of several plant species may represent a nitrogen source for nectarivorous pollinators (Nicolson & Thornburg 2007), as the hummingbirds that feed on the nectar of *Z. montana* flowers.

The disk-stipe was supplied predominantly by phloem, and, probably, the pre-nectar flows away from the sieve tubes through an apoplastic route via intercellular spaces reaching the modified stomata (*e.g*. Wist & Davis 2006). In fact, we observed intercellular spaces filled with flocculent material in the nectary parenchyma tissue of both species. Furthermore, a symplastic pathway of pre-nectar can also occur in the floral nectary via the plasmodesmata, which connects phloem and nectary cells (Wist & Davis 2006; Vassilyev 2010). Additionally, stipe's parenchyma cells presented a peculiar feature, *e.g*. the presence of protuberances along the inner surface of the cell wall, which characterizes them as transfer cells. These protuberances are surrounded by plasma membrane and greatly enlarge the protoplast's surface, favouring transport by apoplast and symplast (Taiz & Zeiger 2013). Transfer cells were reported for several hydrophilic glands such as salt glands and nectaries (Fahn 1979). Moreover, the considerable plastid-juxtaposed mitochondria population observed in these cells is evidence of a secretion mechanism that requires enhanced energy, which is typical of transfer cells (Razem & Davis 1999).

The presence of oil droplets in plastids, inside vacuoles and dispersed in the cytoplasm of the nectary cells of all

tissues and structures suggest that it may participate in the enrichment of floral nectar with lipids (Gilbert & Raven 1975), similar to reported for other Bignoniaceae species (Baker & Baker 1975; Guimarães *et al*. 2016).

The petals axil's cells have a similar subcellular pattern observed in the disk-stipe in both studied species. The presence of amyloplasts with signs of starch grains degradation, rough endoplasmic reticulum and hyperactive Golgi bodies in the petals axil's cells is typical of nectar secreting cells (Fahn 1979; 1988). RER and polyribosomes are evidence of enzymes synthesis that may act in the middle lamellae dissolution (Turner & Croteau 2004), besides contributing to the enrichment of floral nectar. In addition, the epidermal cells' variation in size and shape originates an irregular surface and amplifies the area of nectar release in this region of the nectar chamber. So, the petals' axils seem to have an important role in nectar release, in addition to the modified stomata.

The present study suggests that glandular capitate trichomes are involved in lipophilic secretion, instead of nectar secretion, as previously reported by Bittencourt & Semir (2004). The extensive development of plastids containing tubular osmiophilic structures and electron-dense droplets, together with the proliferation of smooth endoplasmic reticulum, have been described in many lipophilic secretory structures, particularly in those secreting terpenes (Cheniclet & Carde 1985; Figueiredo & Pais 1994; Ascensão *et al*. 1997; Monteiro *et al*. 1999; Turner *et al*. 1999; Machado *et al*. 2006; Possobom *et al*. 2015; Sá-Haiad *et al*. 2015). Terpenes were histochemicaly detected in capitate glandular trichomes in both *Zeyheria* species, which may participate in the attraction of mutualists or in the deterrence of antagonists (Harborne 1997; Nishida 2002; Raguso 2004; Machado *et al*. 2006; Guimarães *et al*. 2008).

The presence of polyribosomes, Golgi bodies and rough endoplasmic reticulum elements in these cells can be related to the increased cytoplasmic enzyme synthesis needed for cell metabolism and terpene biosynthesis (Turner & Croteau 2004). Furthermore, such organelles are also associated to the synthesis of the pectinases and cellulases involved in the wall degradation processes during the subcuticular space development (Ascensão *et al*. 1997; Machado *et al*. 2006). In fact, in both studied species, we observed sinuous, loose walls together with cuticle detachment in the head secretory cells.

Some papillae ultrastructural features from both *Zeyheria* species, such as abundant cytoplasm with modified plastids, abundance of RER, and presence of osmiophilic drops and protein bodies are consistent with secretion activity. We believe that the osmiophilic inclusions observed in the plastids, cytoplasm and vacuoles may be flavonoids, since these compounds were histochemically identified in the papillae. Flavonoids are a remarkably diverse group of polyphenolic secondary metabolites with a vast array of biological functions, such as defense against pathogenes, cell cycle inhibition, chemical messengers, control of auxin transport and stress protection (Roshchina & Roshchina 1993; Petrussa *et al*. 2013). Flavonoids are synthesized by a cytosolic multienzyme complex loosely associated to membranes of different organelles, such as the cytoplasmic face of the endoplasmic reticulum, vacuoles, plastids and nucleus (Petrussa *et al*. 2013). We hypothesize that the papillae contributes, in some way, for nectar secretion or nectar enrichment.

This study showed that all structures and tissues of the nectar chamber have secretory activity and we suggest that, in some way, all of them are involved in nectar secretion, characterizing a complex and integrated system of floral nectar production in *Zeyheria* species. This kind of nectary system is a novelty, since it comprises several tissues and structures functioning in an integrated fashion. Thus, in spite of its reduction in size, the disk is functional in nectar secretion in both *Zeyheria* species. This finding contradicts the previous general assumptions that reduced disks in Bignoniaceae are non-functional in nectar secretion. Therefore, the use of routine methods together with ultracytochemical techniques in transmission electron microscopy allowed us to investigate more accurately the relationship between cell structure and function. Our results highlight the importance of detailed cytological and cytochemical studies in order to assess the functionality of floral nectaries with different developmental degrees in Bignoniaceae. Therefore, other Bignoniaceae genera are under study to verify if our findings on *Zeyheria* genus can be extended to other species with reduced nectary disk.

Acknowledgements

This work was supported by 'Fundação de Amparo à Pesquisa do Estado de São Paulo' [Biota Program Proc. 2008/55434-7; PD-Fellowship to E. Guimarães, Proc. 2009/17611-7]; the 'Conselho Nacional de Desenvolvimento Científico e Tecnológico' [grant to S.R. Machado, scholarship to C. Vaz and Edital MCT/CNPq Proc. 470649/2008-9]. We thank the staff of the Electron Microscopy Centre of the Institute of Bioscience of Botucatu, UNESP – Univ. Estadual Paulista and "Ecology and Evolution of Plant-Animal Interactions" laboratory's students for the field support.

References

Agostini K, Sazima M, Galetto L. 2011. Nectar production dynamics and sugar composition in two *Mucuna* species (Leguminosae, Faboideae) with different specialized pollinators. Naturwissenschaften 98: 933-942.

Alcantara S, Lohmann LG. 2010. Evolution of floral morphology and pollination system in Bignonieae (Bignoniaceae). American Journal of Botany 97: 782-796.

Ascensão L, Marques N, Pais MS. 1997. Peltate glandular trichomes of *Leonotis leonorus* leaves: ultrastructure and histochemical characterization of secretions. International Journal of Plant Sciences 158: 249-258.

Baker HG, Baker I. 1975. Studies of nectar-constitution and pollinator-plant coevolution. In: Gilbert LE, Raven PH. (eds.) Coevolution of animals and plants. New York, Columbia University Press. p. 126-152.

Baker HG, Baker I. 1983. A brief historical review of the chemistry of floral nectar. In: Bentley B, Elias TE. (eds.) The biology of nectaries. New York, Columbia University Press. p 126-152.

Bernardello G. 2007. A systematic survey of floral nectaries. In: Nicolson SW, Nepi M, Pacini E. (eds.) Nectaries and nectar. Dordrecht, Springer. p. 19-128.

Beutler R. 1935. Nectar. Bee World 34: 106-116.

Bittencourt NS, Semir J. 2004. Pollination biology and breeding system of *Zeyheria montana* (Bignoniaceae). Plant Systematics and Evolution 247: 241-254.

Canto A, Pérez R, Medrano M, Castellanos MC, Herrera CM. 2007. Intra-plant variation in nectar sugar composition in two *Aguilegia* species (Ranunculaceae): contrasting patterns under field and glasshouse conditions. Annals of Botany 99: 653-660.

Charrière-Ladreix Y. 1976. Répartition intracellulaire du secrétat flavonique de *Populus nigra* L. Planta 129: 167-174.

Cheniclet C, Carde JP. 1985. Presence of leucoplasts in secretory cells and of monoterpenes in the essential oil: a correlative study. Israel Journal of Botany 34: 219-238.

David R, Carde JP. 1964. Coloration differentielle des pseudophylles de *Pin maritime* au moyen du reactif de Nadi. Comptes Rendus de l'Academie des Sciences 258: 1338-1340.

Evert RF. 2006. Esau's plant anatomy: meristems, cells, and tissues of the plant body: their structure, function, and development. New Jersey, John Wiley & Sons.

Fahn A. 1979. Secretory tissues in plants. London, Academic Press.

Fahn A. 1988. Secretory tissues in vascular plants. New Phytologist 108: 229-257.

Fakan S. 2004. Ultrastructural cytochemical analyses of nuclear functional architecture. European Journal of Histochemistry 48: 5-14.

Figueiredo AC, Pais MS. 1994. Ultrastructural aspects of glandular cells from the secretory trichomes from the cell suspension cultures of *Achillea millefolium L.* ssp. *millefolium*. Annals of Botany 74: 179-190.

Galetto L. 1995. Nectary structure and nectar characteristics in some Bignoniaceae. Plant Systematics and Evolution 196: 99-121.

Galetto L. 2009. Nectary and nectar features: occurrence, significance, and trends in Bignoniaceae. The Journal of Plant Reproductive Biology 1: 1-12.

Galetto L, Bernardello G. 2005. Nectar. In: Dafni A, Kevan PG, Husband BC. (eds.) Pollination ecology: a practical approach. Ontario, Enviroquest. p. 156-212.

Gentry AH. 1974. Coevolutionary patterns in Central American Bignoniaceae. Annals of the Missouri Botanical Garden 61: 728-759.

Gentry AH. 1980. Bignoniaceae. Part I. (Crescentieae and Tourrettieae). Flora Neotropica 25: 1-130.

Gentry AH. 1992. Bignoniaceae. Tribe Tecomeae. Flora Neotropica, Monographs 25, part II. Missouri Botanical Garden Bignonieae (Bignoniaceae). Annals of the Missouri Botanical Garden 99: 348-489.

Gilbert LE, Raven PH. 1975. Coevolution of animals and plants. Austin, University of Texas Press.

González-Teuber, M, Heil M. 2009. Nectar chemistry is tailored for both attraction of mutualists and protection from exploiters. Plant Signaling & Behaviour 4: 809-813.

Guimarães E, Stasi LC, Maimoni-Rodella RCS. 2008. Pollination biology of *Jacaranda oxyphylla* with an emphasis on staminode function. Annals of Botany 102: 699-711.

Guimarães E, Nogueira A, Machado SR. 2016. Floral nectar production and nectary structure of a bee-pollinated shrub from Neotropical savannah. Plant Biology 18: 26-36.

Harborne JB. 1997. Plant secondary metabolism. In: Crawley MJ. (ed.) Plant ecology. 2nd. edn. Berlin, Blackwell Publishing. p. 132-155.

Herrera CM, Pérez R, Alonso C. 2006. Extreme intra-plant variation in nectar sugar composition in an insect-pollinated perennial herb. American Journal of Botany 93: 575-581.

Johansen DA. 1940. Plant microtechnique. New York, McGraw-Hill.

Lohmann LG, Taylor CM. 2014. A new generic classification of tribe Bignonieae (Bignoniaceae). Annals of Missouri Botanical Garden 99: 348-489.

Lopes AV, Vogel S, Machado IC. 2002. Secretory trichomes, a substitutive floral nectar in *Lundia* A. DC. (Bignoniaceae), a genus lacking a functional disc. Annals of Botany 90: 169-174.

Machado SR, Gregório, EA, Guerreiro SMC. 1995. Ultrastructural aspects of the peltate glandular trichomes of the gynoecium in *Zeyheria digitalis* (Vell.) Hoehne (Bignoniaceae). Revista Brasileira de Botânica 18: 197-205.

Machado SR, Gregório EA, Guimarães E. 2006. Ovary peltate trichomes of *Zeyheria montana* (Bignoniaceae): developmental ultrastructure and secretion in relation to function. Annals of Botany 97: 357-369.

Mazia D, Brewer PA, Alfert M. 1953. The cytochemistry staining and measurement of protein with mercuric bromophenol blue. Biology Bulletin 104: 57-67.

Monteiro WR, Fahn A, Caldeira W, Castro MM. 1999. Ultrastructural observations on the foliar secretory cavities of *Porophyllum lanceolatum* DC. (Asteraceae). Flora 194: 113-126.

Nepi M. 2007. Nectary structure and ultrastructure. In: Nicolson SW, Nepi M, Pacini E. (eds.) Nectaries and nectar. Dordrecht, Springer. p. 129-166.

Nepi M, Aderkas P, Wagner R, Mugnaini S, Coulter A, Pacini E. 2009. Nectar and pollination drops: how different are they? Annals of Botany 104: 205-219.

Nicolson SW, Thornburg RW. 2007. Nectar chemistry. In: Nicolson SW, Nepi M, Pacini E. (eds.) Nectaries and nectar. Dordrecht, Springer. p. 129-166.

Nishida R. 2002. Sequestration of defensive substances from plants by Lepidoptera. Annual Review of Entomology 47: 57-92.

O'Brien TP, Feder N, McCully ME. 1964. Polychromatic staining of plant cell walls by toluidine blue. Protoplasma 59: 368-373.

Pacini ENMVJ, Nepi M, Vesprini JL. 2003. Nectar biodiversity: a short review. Plant Systematics and Evolution 238: 7-21.

Petrussa E, Braidot E, Zancani M, *et al*. 2013. Plant flavonoides: biosynthesis, transport, and involvement in stress response. International Journal of Molecular Sciences 14: 14950-14973.

Possobom CCF, Guimarães E, Machado SR. 2015. Structure and secretion mechanisms of floral glands in *Diplopterys pubipetala* (Malpighiaceae), a neotropical species. Flora 211: 26-39.

Pryce-Jones J. 1944. Some problems associated with nectar, pollen, and honey. Proceedings of the Linnean Society of London 155: 129-174.

Purvis MJ, Collier DC, Walls D. 1964. Laboratory techniques in botany. Washington, Butterworth.

Raguso RA. 2004. Why are some floral nectar scented? Ecology 85: 1486-1494.

Razem FA, Davis AR. 1999. Anatomical and ultrastructural changes of the floral nectary of *Pisum sativum* L. during flower development. Protoplasma 206: 57-72.

Reinecke M, Walther C. 1978. Aspects of turnover and biogenesis of synaptic vesicles at locust neuromuscular junctions as reveled by iodide-osmium tetroxide (ZIO) reacting with intravesicular sh-groups. Journal of Cell Biology 21: 839-855.

Reynolds ES. 1963. The use of lead citrate at high pH as an electron-opaque stain in electron microscopy. Journal of Cell Biology 17: 208-212.

Rivera GL. 2000. Nuptial nectary structure of Bignoniaceae of Argentina. Darwiniana 38: 227-239.

Rizzini CT. 1997. Tratado de fitogeografia do Brasil: aspectos ecológicos, sociológicos e florísticos. Rio de Janeiro, Âmbito Cultural Edições Ltda.

Robards AW. 1978. An introduction to techniques for scanning electron microscopy of plant cells. In: Hall JL. (ed.) Electron microscopy and cytochemistry of plant cells. New York, Elsevier. p. 343-415.

Roshchina VV, Roshchina VD. 1993. Excretory function of higher plants. Berlin, Springer-Verlag.

Sá-Haiad B, Silva CP, Paula RC, Rocha JF, Machado SR. 2015. Androecia in two *Clusia* species: development, structure and resin secretion. Plant Biology 17: 816-824.

Smets E. 1986. Localization and systematic importance of the floral nectaries in the Magnoliatae (Dicotyledons). Bulletin du Jardin botanique national de Belgique/Bulletin van de Nationale Plantentuin van Belgie 56: 51-76.

Souza CV. 2015. Biologia floral de *Zeyheria tuberculosa* (Bignoniaceae). MSc Thesis, Universidade Estadual Paulista, Brazil.

Svendsen AB, Verpoorte R. 1983. Chromatography of alkaloids. New York, Elsevier Scientific Publishing Company.

Taiz L, Zeiger E. 2013. Fisiologia vegetal. 5th. edn. Porto Alegre, Artmed.

Thomas V, Dave Y. 1992. Structure and biology of nectaries in *Tabebuia serratifolia* Nichols (Bignoniaceae). Botanical Journal of the Linnean Society 109: 395-400.

Turner GW, Croteau R. 2004. Organization of monoterpene biosynthesis in *Mentha*. Immunocytochemical localizations of geranyl diphosphate synthase, limonene-6-hydroxylase, isopiperitenol dehydrogenase, and pulegone reductase. Plant Physiology 136: 4215-4227.

Turner G, Gershenzon J, Nielson EE, Froehlich JE, Croteau RB. 1999. Limonene synthase, the enzyme responsible for monoterpene biosynthesis in peppermint, is localized of oil gland secretory cells. Plant Physiology 120: 879-886.

Vassilyev AE. 2010. On the mechanisms of nectar secretion: revisited. Annals of Botany 105: 349-354.

Vogel S. 1997. Remarkable nectaries: structure, ecology, organophyletic perpectives. I. Substitutive nectaries. Flora 192: 305-333.

Wilmer P. 2011. Pollination and floral ecology. Princeton, Princeton University Press.

Wist TJ, Davis AR. 2006. Floral nectar production and nectary anatomy and ultrastructure of *Echinacea purpurea* (Asteraceae). Annals of Botany 97: 177-193.